

Elaboration and Characterization of SnO_2 synthesis by Sol-Gel Method for PLA Polymer Reinforcement

Rahima Zellagui¹, Fayssal Boufelgha², Mohamed Cherif Benachour³, Heider Dehdouh⁴, Nouredine Brihi⁵, Slimane Hadjab⁶ And Fayçal Labrèche⁷

^{1,2,3,4}Research Center in Industrial Technologies CRTI, P.O.Box 64, Cheraga 16014, Algiers, Algeria

^{2,5,6,7}Laboratoire Physique de la Matière Condensée et Nanomatériaux (LPMCN), Département de Physique, Faculté des Sciences Exactes et Informatique, Université de Jijel, 18000 Algeria

The Author's E-mail: rahima32@hotmail.fr¹, r.zellagui@crti.dz¹, boufelghalem@yahoo.fr², benachour25cherif@gmail.com³, dehdouh.heider@hotmail.fr⁴, nourb_brihi@yahoo.fr⁵, hadjeb Slimane18@gmail.com⁶, faycal_labreche@yahoo.fr⁷

Received: 17/08/2023, Published: 07/12/2023

Abstract:

In recent years, polymer composite materials have become very attractive due to their new properties successfully derived from the combined properties of polymer compounds in a single material. These composite materials are used to reinforce polymers, in particular, to improve their physical and mechanical properties when used in additive manufacturing. In the current work, we have synthesized SnO_2 powder by the solgel technique. The SnO_2 powder prepared was characterized by XRD to have a structure that is polycrystalline and a grain size is around 8.08 nm, absorbance in UV-visible, FTIR to know the chemical band and the morphology of the particles is observed by the MEB. The results showed good structural and optical properties of the prepared SnO_2 powder. for use as reinforcing material of PLA polymer in the future

Keywords: composite materials, UV-visible, Powder, SnO_2 , FTIR, additive manufacturing, Polymer (PLA).

Tob Regul Sci. TM 2023;9(2):1559 - 1568

DOI: doi.org/10.18001/TRS.9.2.97

1- Introduction

In recent years, polymer composite materials have become highly attractive because of their novel properties derived successfully from the combined properties of polymer composites into a single material [1]. Polylactic acid (PLA) is produced from renewable feedstock, and it is one of the most important biobased thermoplastic polyesters due to its renewability, biodegradability and biocompatibility, and mechanical properties compared to polystyrene (PS) [2]. PLA is rapidly gaining recognition in various new applications besides biomedical, such as industrial packaging,

the automobile industry, and electronics [3]. The limitations of PLA are its main characteristic brittleness/hardness and low hardness below the glass transition temperature (T_g), and therefore it must be annealed to produce more flexible films. However, plasticized PLA films exhibit poor thermal, mechanical and barrier properties, due to the large amounts of hydrophilic plasticizers such as polyethylene glycol (PEG) required for film flexibility and processability [4]. Research efforts are therefore focused on improving the performance of PLA, mainly by mixing it with other biopolymers or incorporating nanofillers. The incorporation of nanoparticles (NPs) as particulate fillers into polymer matrices is an important technology that can lead to significant improvements in PLA properties (mechanical, thermal, barrier, etc.) [5]. Polymer nanocomposites are made by dispersing inorganic or organic NPs in a thermoplastic polymer or a thermoset polymer. Nanoparticle NPs have been studied for their optical, electronic, electrical, and chemical properties, such as high active area, high stability, wide bandgap, and confinement. With these properties, metal oxide nanoparticles (NPs) are at the center of attention [6]. The increased research interest in SnO_2 nanomaterials is due to their tunable physical and chemical properties [7]. SnO_2 nanoparticles are transparent in the visible range and are highly reflective in the NIR region with a wide energy bandgap (~ 3.64 eV). These are n-type semiconductors due to the presence of oxygen vacancies at room temperature (non-stoichiometry). Besides all these properties, SnO_2 nanomaterials have high chemical and mechanical stability, low cost and environmental friendliness [8]. Hence, these materials find widespread applications as transparent conducting electrodes e.g. solar cells, in optoelectronic devices [9], as gas sensors [10], and as a catalyst for oxidation of solids [11]. Different physical and chemical methods are available for the synthesis of potentially useful tin oxide nanoparticles; these available methods are tedious and pose an environmental threat. It is obvious from the electrical, electronic and structural properties of an atomic cluster of metal oxide NPs how to convert into crystallite size and the size of the NPs can be regulated by the soft chemical synthesis methods [12]. Many methods have been incorporated for the synthesis of SnO_2 NPs, e.g. sol-gel method [13], chemical precipitation [14], hydrothermal method [15], etc. Although apart from various SnO_2 synthesis processes, the sol-gel method offers various advantages over other methods in terms of better homogeneity, high purity, phase-pure powders at lower processing temperatures, controlled stoichiometry and flexible formation of intense monoliths, thin films and NPs.

The main objective of this work is to synthesize sol-gel SnO_2 NPs and their structural, optical and morphological properties, to use them in the reinforcement of PLA polymer for use in additive manufacturing.

2- Experimental

SnO_2 NPs were synthesized via the sol-gel method; Precursor materials used included Tin chloride ($\text{SnCl}_2 \cdot \text{H}_2\text{O}$) ($\text{C}_2\text{H}_5\text{OH}$), and monoethanolamine ($\text{C}_2\text{H}_7\text{NO}$) as a stabilizer. The

synthesis process is schematically described in Figure 1. After the recovery of nanoparticles, annealing is carried out in a muffle furnace at a temperature of 500°C for 1 hour.

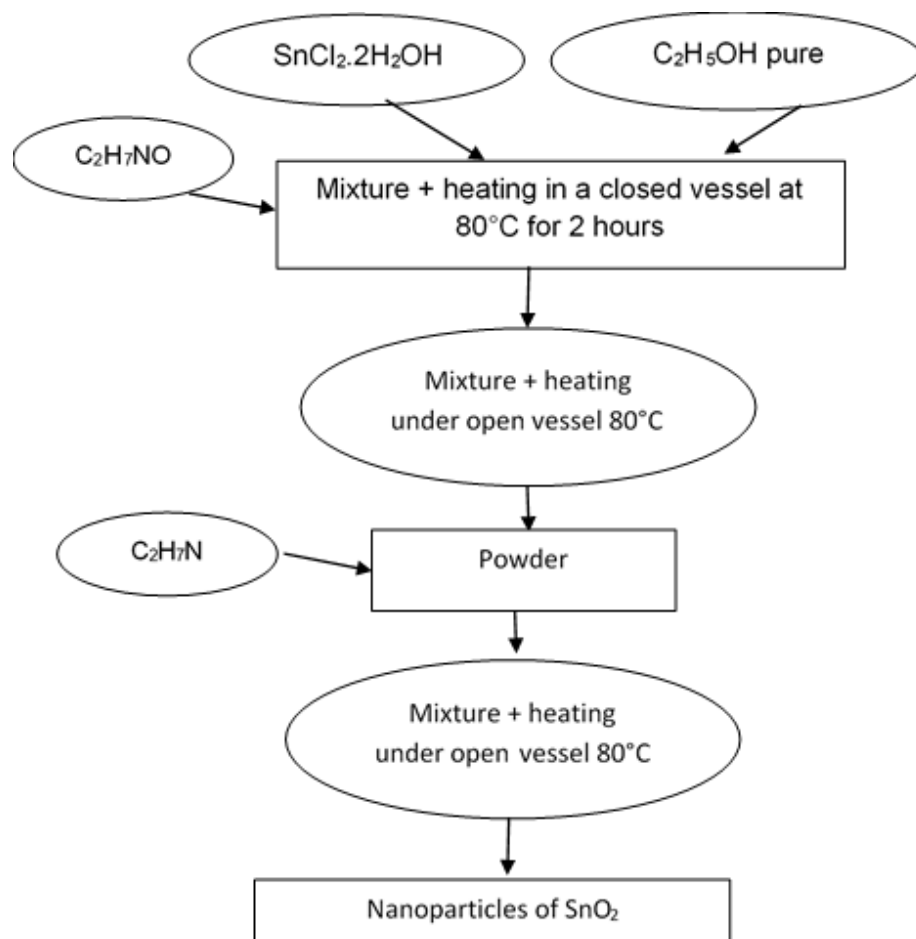


Fig.1. Diagram of the synthesis process.

The structural analysis of samples was performed using a Bruker X-ray diffractometer (D8 Advance) with $\text{CuK}\alpha$ radiation ($\lambda = 1.54 \text{ \AA}$). The absorbance of NPs of SnO_2 over the visible range was recorded by UV-vis Shimadzu UV 2600i Spectrophotometer, FTIR spectrum analysis for functional group identification was done by making pellets of the samples using a Jasco FT/IR 6800 spectrometer and the morphological of nanoparticles were investigated by scanning electronic microscopy JEOL -JCM 5000 NeoScope.

3- Results and discussion

a) Structural proprieties

Figure 2 shows the XRD patterns of the as-prepared powder. All diffraction lines were indexed on the tetragonal structure of SnO_2 ; inconsistent with the reported data (JCPDS file no. 96-152-6638). No traces of unidentified peaks were present in these patterns, which confirms that only pure SnO_2 NPS were obtained. The XRD patterns show broad peaks matching the expected

diffraction reflections of the (110), (101), and (211) corresponding to the tetragonal structure of SnO₂ NPs and Space group (P 42/m n m). The inter-planar spacing of NPs of SnO₂ was estimated using Bragg's equation [16] and produced in the following table:

$$d = \frac{n\lambda}{2\sin \theta} \quad (1)$$

A small difference in d-spacing between the experimental and standard data was observed.

The crystallite size (average) was calculated using the Debye-Scherrer formula [16]:

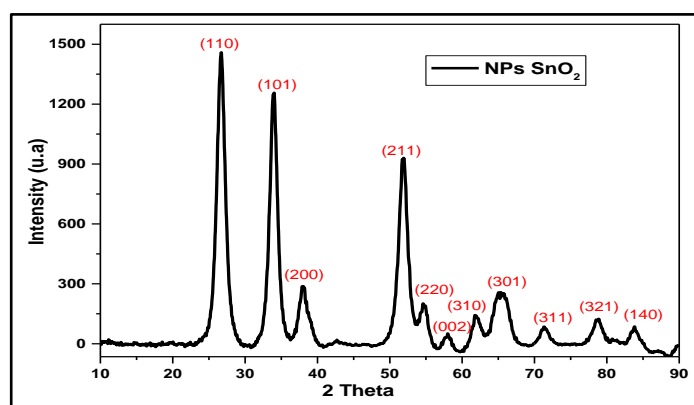
$$D = \frac{0.9\lambda}{\beta \cos \theta} \quad (2)$$

Where "D" represents the crystallite size, λ represents the wavelength of the X-ray, and β represents the full width at half maximum (FWHM).

Table: Structural parameters

2θ	d (Å)	hkl	FWHM	D (nm)	σ (line/m²)	ϵ (%)
26.71	3.33	110	1.0367	8.06	1.53 10 ¹⁸	0.25
33.94	2.63	101	0.93096	8.97	1.24 10 ¹⁸	0.22
38.25	2.35	200	0.88484	9.51	1.10 10 ¹⁸	0.20
51.91	1.75	211	1.0808	7.88	1.61 10 ¹⁸	0.24
54.99	1.66	220	0.7121	12.00	0.69 10 ¹⁸	0.15
57.95	1.58	002	1.2291	6.97	2.05 10 ¹⁸	0.26
61.84	1.49	310	0.88487	9.73	1.05 10 ¹⁸	0.18
65.33	1.42	301	3.5627	2.43	16.93 10 ¹⁸	0.74
71.29	1.32	311	1.2189	7.15	1.95 10 ¹⁸	0.24
78.85	1.21	321	1.2091	7.29	1.88 10 ¹⁸	0.23
83.83	1.15	140	1.0795	8.23	1.47 10 ¹⁸	0.20

The average crystallite size of SnO₂ nanoparticles was found to be approximately 08.08 nm. Results show that the prepared material is pure as no any other peaks are observed in the pattern. The lattice constants of unit cells a and c as well as their cell volume were calculated using tetragonal phase Relations

Fig. 2. XRD patterns of SnO₂ nanoparticles.

$$\frac{1}{d^2} = \frac{h^2 + k^2}{a^2} + \frac{l^2}{c^2} \quad (3)$$

$$V = a^2 c \quad (4)$$

Where d represents interplanar spacing and hkl denotes miller indices of the lattice planes, as we can see that the lattice constants and unit cell volume are very similar to JCPDS values ' $a=b=4.70$ Å, $c=3.16$ Å, and volume $V=69.80$ Å³' of the typical tetragonal rutile structure [17].

b) FT-IR analysis

FT-IR spectroscopy is an important tool for structural elucidation and compound analysis. The FT-IR spectrum of SnO₂ nanoparticles is shown in Figure 3. Three main bands appeared at approximately 3408 cm⁻¹, 1627 cm⁻¹ and 650 cm⁻¹. The stretching vibration corresponding to the pristine Sn–O sample was indicated by the peak at 522 cm⁻¹, while the stretching modes of Sn–O–Sn were indicated by the peak at 640–660 cm⁻¹ [18]. The band around the 1630 cm⁻¹ region is attributed to the bending vibration of the H₂O molecules, confined in the SnO₂ sample. The minimum transmittance on the 3400 cm⁻¹ wavelength is related to the O–H stretching vibration of the adsorbed H₂O molecules.

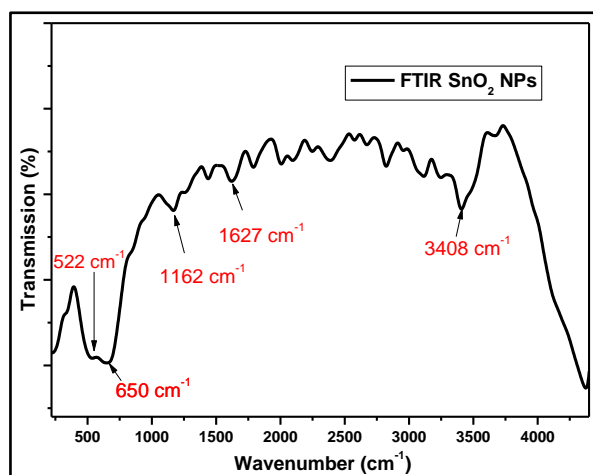
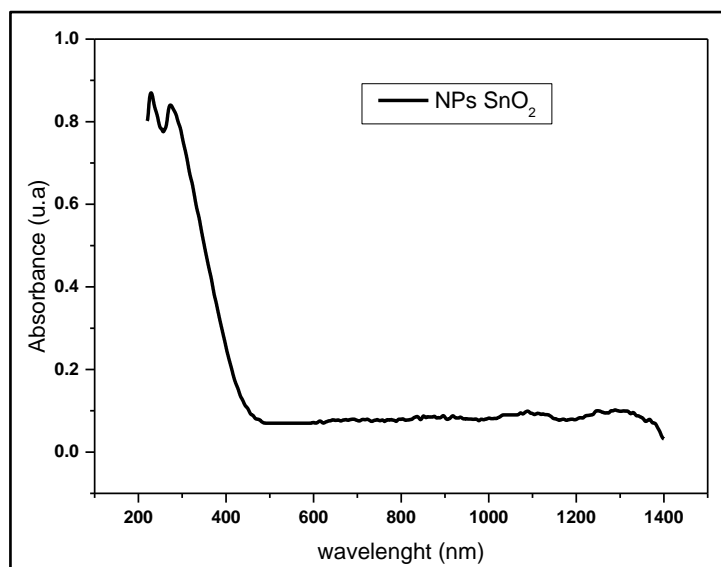


Fig. 3. FTIR spectra of SnO₂ nanoparticles.

c) Optical analysis

The optical absorbance spectrum of the synthesized SnO₂ nanoparticles is recorded in the wavelength range of 200 nm and 1400 nm is shown in Figure. 4. The spectrum shows that a net absorbance is in the wavelength range of about 270 nm and about 450 nm. A similar net absorbance was observed in previous reports on SnO₂ nanoparticles [6].

Fig.4. Absorbance spectra of SnO₂ nanoparticles.

We calculate the bandgap of SnO₂ nanoparticles from UV-visible spectra using the TAUC method. Using the equation $\alpha(h\nu) = A(h\nu - E_g)^n$ where $h\nu$ is the energy of the incident photon. [19]. E_g is the authorized energy difference, A is a constant, $\alpha(h\nu)$ is the absorption coefficient of the Lambert-Beer law and $n = 1/2$ for the authorized direct transition [20].

The following procedure was performed. First, by comparing the TAUC equation and the straight-line equation (Eq. (1) and (2)) setting the y-axis equal to zero will give us the equation of the x-axis. (3), then plot the extrapolation of the first linear region on the x-axis, which will be the bandgap energy Eq. (4).

$$\alpha(h\nu) = A(h\nu - E_g)^n \quad (1)$$

$$y = m(x) \quad (2)$$

$$0 = A(h\nu - E_g) \quad (3)$$

$$h\nu = E_g \quad (4)$$

Figure 5 shows the extrapolating of the linear part of the curve between $(\alpha h\nu)^2$ and photon energy ($h\nu$), the value of the optical bandgap of SnO_2 NPs is 3.4 eV.

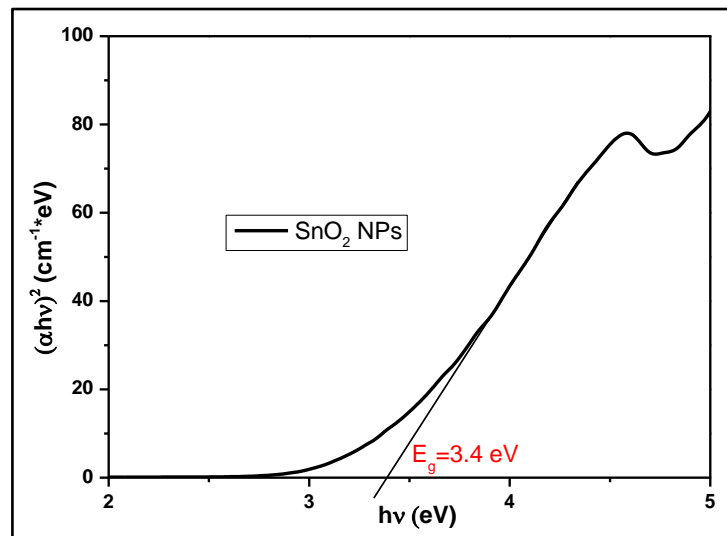


Fig.5. Eg of SnO_2 nanoparticles.

d) Morphological image

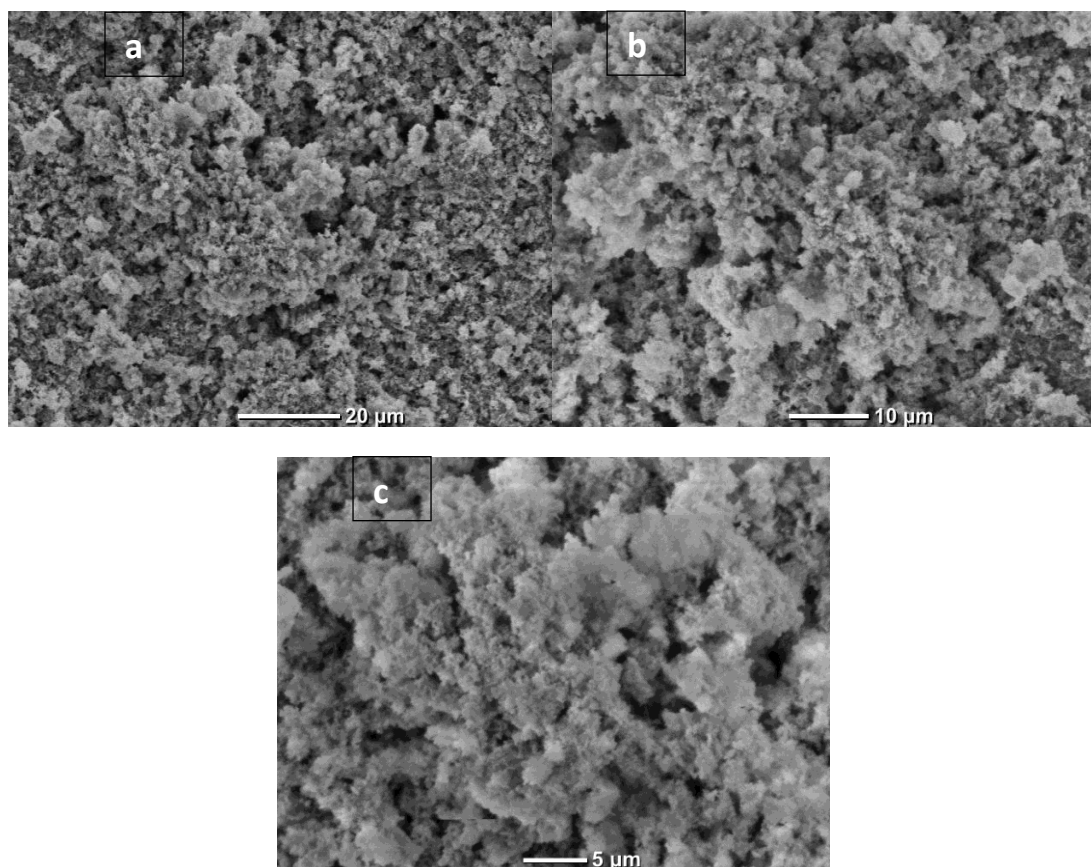


Fig.6. SEM image of SnO_2 nanoparticles.

The SEM images of the SnO_2 nanoparticles synthesized by the sol-gel method at different magnifications are shown in Figure 6 (a, b, c). Detailed analysis of the images indicates the nanoparticles to be formed from the platelets. The formation of nanoparticles is due to sol-gel synthesis at high temperatures [21].

4- Conclusion

Synthesis tin oxide is used as a tin chloride precursor ethanol as a solvent and monoethanolamine as a complexing agent by the sol-gel method. XRD showed that they possessed a SnO_2 phase with a tetragonal unit cell structure. Results show that the prepared material is pure as no any other peaks are observed in the pattern. The average crystallite size determined from XRD was found to be 8.08 nm. absorbance is in the wavelength range of about 270 nm and about 450 nm FTIR analysis of the nanoparticles showed that they were slightly hydrated in nature. The presence of water-bound bonds on the nanoparticles is due to their wet synthesis. The morphology of SnO_2 nanoparticles to be formed from the platelets. These results favor the application of these NPs of SnO_2 in reinforced polymer PLA.

5- Reference

- [1] B. M. Basavaraja Patel, M. Revanasiddappa, D. R. Rangaswamy, Synthesis, Transport, and Electromagnetic Shielding Properties of Fe-PPy- SnO_2 Nanocomposites, Journal of Electronic Materials (2022) 51:6937–6950
- [2] L.T. Lim, R. Auras, M. Rubino, Processing Technology for Poly(lactic acid), Progress in Polymer Science. 33(2008) 820-852.
- [3] A.R. Boccaccini, I. Notingher, V. Maquet, R. Jérôme, Bioresorbable and bioactive composite materials based on polylactide foams filled with and coated by Bioglass® particles for tissue engineering applications. Journal of Materials Science: Materials in Medicine 14(2003) 443-450.
- [4] Jasim Ahmed, Yasir Ali Arfat, Edgar Castro-Aguirre, Rafael Auras, Mechanical, structural and thermal properties of Ag-Cu and ZnO reinforced polylactide nanocomposite films, International Journal of Biological Macromolecules, 86 (2016) 885-892
- [5] J. Ahmed, S.K. Varshney, R. Auras, Rheological and Thermal Properties of Polylactide/Silicate Nanocomposites Films, J. Food Sci. 75 (2010) N17-N24.
- [6] Sk. I. Ali, D. Dutta, A. Das, S. Mandal, A. C. Mandal, Understanding the structure-property correlation of tin oxide nanoparticles synthesized through the sol-gel technique, Journal of Luminescence 253 (2023) 119465 (1-13)

- [7] X. Luo, W. Cao, L. Zhou, Synthesis and luminescence properties of (Zn, Cd) S: Ag nanocrystals by hydrothermal method, *J. Lumin.* 122 (2007) 812–815.
- [8] M. Chauhan, V. K. Singh, Tapered MMF sensor fabrication using SnO_2 -NPs for alcohol sensing application, *Optical Fiber Technology* 75 (2023) 103167 (1-7)
- [9] V. Kumar, K. Singh, A. Kumar, M. Kumar, K. Singh, A. Vij, A. Thakur, Effect of solvent on crystallographic, morphological and optical properties of SnO_2 nanoparticles, *Mater. Res. Bull.* 85 (2017) 202–208.
- [10] G. Korotcenkov, B.K. Cho, V. Brinzari, L.B. Gulina, V.P. Tolstoy, Catalytically active filters deposited by SILD method for inhibiting sensitivity to ozone of SnO_2 -based conductometric gas sensors, *Ferroelectrics* 459 (2014) 46–51.
- [11] U.Z. Felde, M. Haase, H. Weller, Electrochromism of highly doped nanocrystalline SnO_2 : Sb, *J. Phys. Chem. B* 104 (2000) 9388–9395.
- [12] J.P. Cronin, T.J. Gudgel, S.R. Kennedy, A. Agrawal, D.R. Uhlmann, Electrochromic glazing, *Mater. Res.* 2 (1999) 1–9.
- [13] G. H. Patel, S. H. Chaki, R. M. Kannaujiya, Z. R. Parekh, A. B. Hirpara, A. J. Khimani, M.P. Deshpande, Sol-gel synthesis and thermal characterization of SnO_2 nanoparticles, *Physica B* 613 (2021) 412987 (1-9)
- [14] D. Yu, D. Wang, W. Yu, Y. Qian, Synthesis of ITO nanowires and nanorods with corundum structure by a co-precipitation-anneal method, *Mater. Lett.* 58 (2004) 84–87,
- [15] G. Sakai, N.S. Baik, N. Miura, N. Yamazoe, Gas sensing properties of tin oxide thin films fabricated from hydrothermally treated nanoparticles: dependence of CO and H_2 response on film thickness, *Sensor. Actuator. B Chem.* 77 (2001) 116–121
- [16] A. Y. Abdel-latif, M. A. Abdel-Rahim, N. M. Shaalan, D. Hamad, Structural and crystal growth kinetics studies for SnO_2 nanoparticles prepared via hydrothermal route, phase transitions, 2017.
- [17] S. Blessi, A. Manikandan, S. Anand, M. Maria Lumina Sonia, V. Maria Vinosel, A. Mohamed Alosaimi, A. Khan, M. Ali Hussein, A. M. Asiri, Enhanced electrochemical performance and humidity sensing properties of Al^{3+} substituted mesoporous SnO_2 nanoparticles, *Physica E* 133 (2021) 114820 (1-13)
- [18] M. Akhyar Farruck, Prisca Tan, R. Adnan, Surfactant-controlled aqueous synthesis of SnO_2 nanoparticles via the hydrothermal and conventional heating methods, *Turk. J. Chem.* 36(2010) 303–314.

- [19] P. Makula, M. Pacia, W. Macyk, How to correctly determine the band gap energy of modified semiconductor photocatalysts based on UV-Vis spectra, *J. Phys. Chem. Lett.* 9 (2018) 6814–6817.
- [20] J. Sahu, S. Kumar, V.S. Vats, P.A. Alvi, B. Dalela, S. Kumar, S. Dalela, Lattice defects and oxygen vacancies formulated ferromagnetic, luminescence, structural properties and band-gap tuning in Nd³⁺ substituted ZnO nanoparticles, *J. Lumin.* 243 (2022) 118673.
- [21] Gauravkumar H. Patel, Sunil H. Chaki, Rohitkumar M. Kannaujiya, Zubin R. Parekh, Anilkumar B. Hirpara, Ankurkumar J. Khimani, M.P. Deshpande, Sol-gel synthesis and thermal characterization of SnO_2 nanoparticles, *Physica B* 613 (2021) 412987.